Contents

1 Introduction

1.1 Context

The simulation of infectious diseases over complex networks serves as a powerful tool to understand the dynamics of epidemics and assess the impact of various network structures on disease spread. In this lab assignment, we delve into the realm of the Susceptible-Infectious-Susceptible (SIS) model, a widely used framework for studying the transmission dynamics of infectious diseases within populations. The goal is to validate the epidemic threshold, denoted as λ_1 and predicted by [1], for arbitrary networks.

The SIS model considers nodes within a network as individuals, with each node having two possible states: susceptible or infected. At each time step, the infected nodes have a chance to recover, while trying to infect their neighbors with certain probabilities, denoted γ and β, respectively. Updates to the statuses of the nodes occur in parallel, ensuring that the statuses at time t only depend on the statuses at time t-1 of the other nodes.

1.2 This work

The focus of this simulation is on networks of size n = 1000, encompassing various network models such as Erdös-Rényi random graphs (ER), Barábasi-Albert scale-free networks (BA) and Watts-Strogatz small world networks (WS). Additionally, two other network models will be explored: trees and star networks.

The tasks involve running simulations with fixed sets of γ, β and initial infection fraction (p_0) values, studying the proportion of infected nodes over time for each network. The objective is to identify networks that exhibit varying propensities for epidemic outbreaks. A key aspect of the analysis involves calculating the leading eigenvalue of each network to gain insight into its structural characteristics and relate them to the observed epidemic behavior.

Additionally, the assignment involves determining the epidemic threshold for each type of network. Two sets of parameter values for γ and β, one slightly above and one slightly below the threshold, will be chosen to simulate the spread of the disease. The results will be compared with theoretical expectations, providing insight into the consistency between the simulation outcomes and the established epidemiological theories.

Through this comprehensive exploration of different network structures and their impact on disease spread, our aim is to improve our understanding of complex network epidemiology and validate the theoretical predictions

associated with the SIS model.

2 First Exercise

2.1 Methodology

We will study the behaviour of the evolution of an epidemic on graphs constructed using the following five different models:

- Erdös-Renyi model
- Barabási-Albert model
- Small-World or Watts-Strogatz model
- Star
- Tree

Two sets of experiments have been carried out.

- The first experiment consisted of plotting the spread of the epidemic with a recovery probability of $\gamma = 0.30$, a spread probability of $\beta = 0.40$ and different percentages of infected nodes initially, $p_0 \in \{0.1, 0.25, 0.5, 0.75, 0.9\}$. Then we compared the result obtained with the leading eigenvalue for each network.
- In the second experiment, we try to observe the variability of the leading eigenvalues on nondeterministic random networks in order to validate the results obtained in the previous experiment and the following task.

All experiments have been performed with 10 repetitions in order to reduce the noise produced by the random nature of the epidemic simulation.

In order to improve the performance of the simulation, instead of spreading from the infectious nodes to the susceptible nodes, we checked what the probability of a node being infected given the number of infectious neighbors is. It was obtained from the following formula:

$$\begin{aligned} P(v_{t+1} = \text{Infected} | v_t = \text{Susceptible}) &= \bigcup_{u \in N(v)} P(Spread of u_t) \\ &= 1 - \bigcap_{u \in N(v)} 1 - P(Spread of u_t) \\ &= 1 - (1-\beta)^{|N(v) \cap \text{Infected}|} \end{aligned}$$

That means that we can simply know the probability of a node to get infected by knowing how many of its neighbours are infected.

2.2 Results

In figure 1, we can observe how all the tested networks evolve with an initial proportion of 25% of the infected nodes. In Appendix A, we can observe the same results of the experiments, but with a percentage of 10%, 25%, 50%, 75% and 90%.

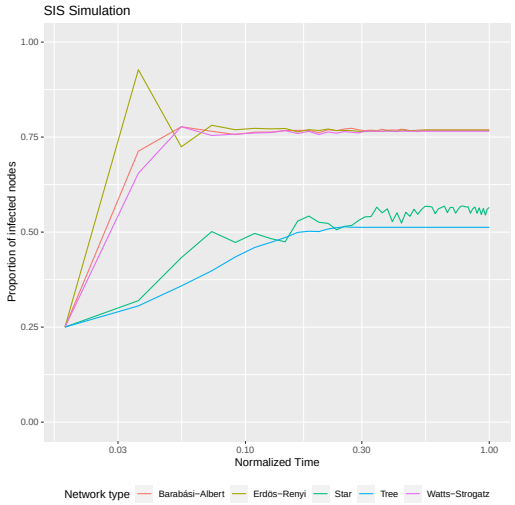

Figure 1: Evolution of the spread for all the tested networks with $\gamma = 0.30, \beta = 0.40, p_0 = 0.25$

We can observe that in all networks the pandemic continues to spread until it reaches a saturation point. This saturation point does not depend on the initial proportion of infected nodes, as can be seen in the Appendix A. If we observe the leading eigenvalue of each network (Table 1), our beta is always above all thresholds, and therefore we expected to have a pandemic. It is remarkable that Erdös-Renyi, Barbási-Albert, and Watts-Strogatz have a faster start than the Star and Tree networks. We could not relate this behavior to the leading eigenvalue because the Star network has a higher eigenvalue than Watts-Strogatz, but it does not have a faster start.

Network	Leading Eigenvalue	Threshold
Erdös-Renyi	399.5150002	0.00075091
Barabási-Albert	29.9042477	0.01003202
Watts-Strogatz	10.4933208	0.02858961
Tree	3.5769977	0.08386922
Star	31.6069613	0.00949158

Table 1: Leading Eigenvalues of each network and the threshold for beta

Because the threshold for beta depends on the leading eigenvalue, which depends on the network, we studied how much it varies. In Appendix B, we show the boxplot of several repetitions in which we generated a graph and checked its leading eigenvalue. First, we observe that all the eigenvalues have a small variation, which allows us to corroborate the previous results. Moreover, we found remarkable that the leading eigenvalue in Erdös-Renyi networks is very close to the expected number of vertices, with really little variation. We also found interesting that the number of children per node in a Tree network does not vary the leading eigenvalues.

3 Second Exercise

3.1 Methodology

We have modeled the evolution of an epidemic spread for the same kind of network as in the previous task. For all of them, we have plotted the evolution of the epidemic when the relation between β, γ is slightly above and below the theoretical epidemic threshold. The theoretical epidemic threshold states whether the infection dies out over time or survives and becomes an epidemic. Chakrabarti et al. empirically observed in [1] that such a

relation is indeed:

$$\frac{\beta}{\gamma} = \frac{1}{\lambda_1}$$

with λ_1 being the leading eigenvalue. Therefore, we have fixed some values of γ and calculated $\beta = \frac{\beta}{\lambda_1} + \varepsilon, \varepsilon \in \{-0.05, 0.05\}$, in order to analyze whether the epidemic threshold was the expected one for each network. Because, if the relation is above, we expect the epidemic to occur; and if the relation is below, we expect no epidemic to occur.

Moreover, we have used a set of different values for γ and the parameters that allow us to define the different networks such as:

- In the Erdös-Renyi model, the expected density
- In the Barbási-Albert model, the number of clusters
- In the Watts-Strogatz model, the rewiring probability
- In the Tree model, the number of children per node

The set of values used for γ are:

$$\gamma \in \{0.15, 0.3, 0.45, 0.6, 0.75, 0.9\}$$

All experiments have been performed with 10 repetitions in order to reduce the noise produced by the random nature of the epidemic simulation.

3.2 Results

In the following appendices, we present the outcomes obtained from various network models. Specifically, Appendix C showcases the results from the Erdös-Renyi model, while Appendix D displays the outcomes from the Barbäsi-Albert model. Additionally, Appendix E provides the results for the Watts-Strogatz model, Appendix F presents the outcomes of the Star model, and Appendix G exhibits the results for the Tree model.

Results show that, in general, in the first case (case where the previously mentioned relation is slightly higher than threshold), the number of infected nodes grows until it reaches a stabilization point, meaning that the infection becomes an epidemic with a stable rate of infected nodes or saturation point, which is different for each type of graph, while in the second case (case where the previously mentioned relation is slightly lower than threshold) shows that the number of infected nodes drops to zero, meaning the infection dies and therefore does not turn into an epidemic.

This behavior can be observed for all values of γ and different configurations of the networks that have been used in these experiments, supporting the existence of this theoretical threshold in complex networks such as those that define social interconnections in real life.

From plots in C, D and E, one can observe that the higher γ, the less time it takes to reach the death point of the infection, when we are below the epidemic threshold. However, the higher γ, the longer it takes to reach equilibrium or convergence in the number of infected nodes, and a higher number of infected nodes will be required to reach the expected saturation point. Additionally, it is worth mentioning that as the value of γ increases, the equilibrium point decreases. On the other hand, we observed that the magnitude of the leading eigenvector does not seem to be as determinant as γ.

The deterministic models of graph generation demonstrate a similar behavior to the random models in terms of the spread of the epidemic. The epidemic threshold can be determined from the plots in Appendix F and Appendix G. These plots indicate that the networks generated using deterministic models tend to restrict the spread of infections to a smaller expected number of infected nodes. This can be attributed to the specific structural properties of these graphs, leading to different patterns of epidemic spread.

In a tree graph, the absence of cycles implies a hierarchical structure with a unique path from the root to any node. This hierarchical arrangement often results in a linear spread of infection. Each node in the tree has only one direct path to the source of infection, and, as a consequence, the infection tends to spread linearly along the branches of the tree, causing a smaller percentage of infected nodes (almost zero when the recovery probability is high). Furthermore, since nodes in a tree have fewer connections compared to random graphs, the potential for widespread transmission is limited. This results in a slower and more localized epidemic spread.

In a star graph, all peripheral nodes are directly connected to a central node. The central node plays an important role in the transmission of infection to the periphery. The infection can spread only through two routes: from the central node to the peripheral nodes and vice versa. This limited set of transmission routes restricts the overall spread of the epidemic.

From these observations some interesting conclusions can be inferred:

- The experimental validation of the theoretical epidemic threshold demonstrates its existence across a range of graphs, created through the use of either random or deterministic models. Notably, there is no discernible difference between these graph types in terms of the existence of an epidemic threshold, as all consistently manifest its inherent presence due to obvious behavior differences, such as infection's extinction when experiments have taken place below this threshold or infection evolution into epidemic when experiments have taken place above this threshold.
- In the context of infection dynamics, the relation between γ and β plays a predominant role, overshadowing the impact of the configuration of the type of network.
- Structural characteristics of tree and star graphs, such as linear spread in trees and centralized connectivity in stars, contribute to a more localized and constrained epidemic spread compared to the more interconnected and random nature of graphs like Erdös-Renyi, Barabási-Albert, and Watts-Strogatz. These insights into the relationship between graph structure and epidemic dynamics are valuable for understanding how network topology influences the transmission of infectious diseases and can inform strategies for disease control and prevention.

References

[1] Deepayan Chakrabarti, Yang Wang, Chenxi Wang, Jurij Leskovec, and Christos Faloutsos. "Epidemic thresholds in real networks". In: *ACM Transactions on Information and System Security* 10.4 (Jan. 2008), pp. 1–26. ISSN: 1557-7406. DOI: 10.1145/1284680.1284681. URL: http://dx.doi.org/10.1145/1284680.1284681.

A All models with $\gamma = 0.3$ and $\beta = 0.4$

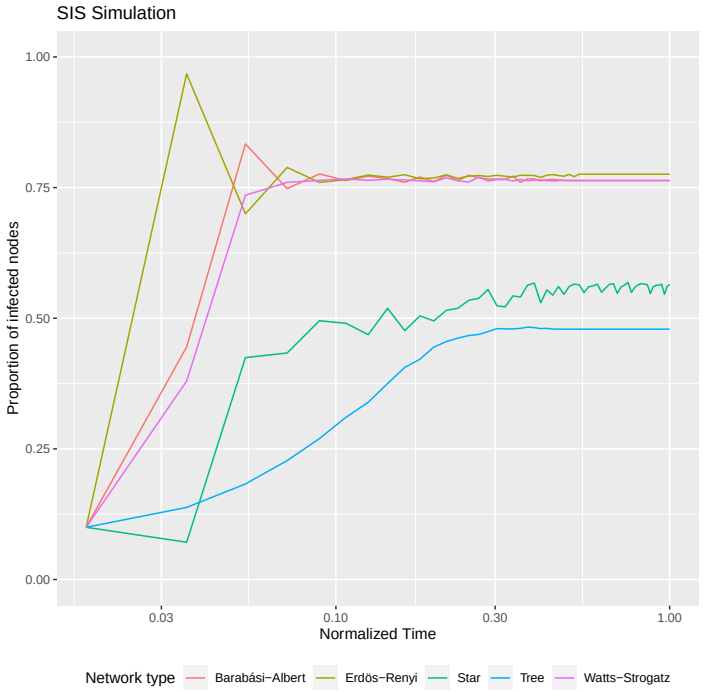

Figure 2: All networks with an initial infected population of 0.10

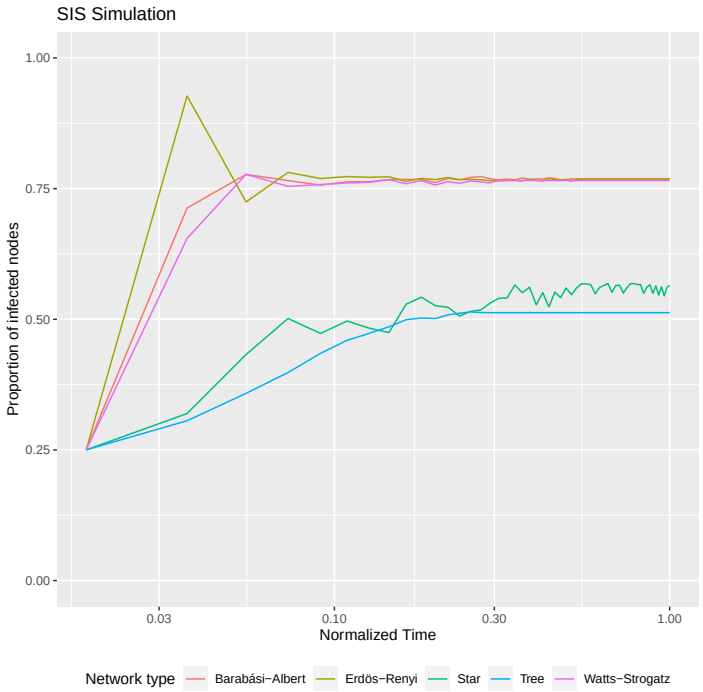

Figure 3: All networks with an initial infected population of 0.25

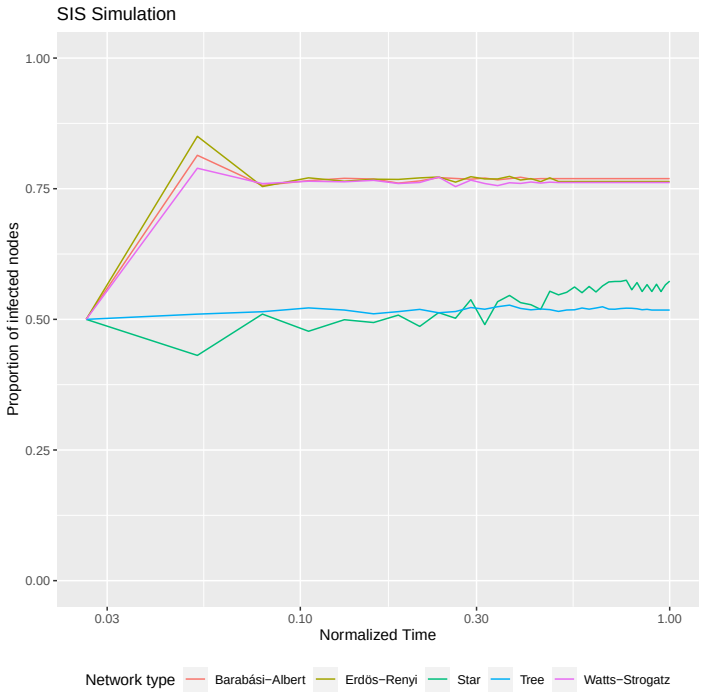

Figure 4: All networks with an initial infected population of 0.50

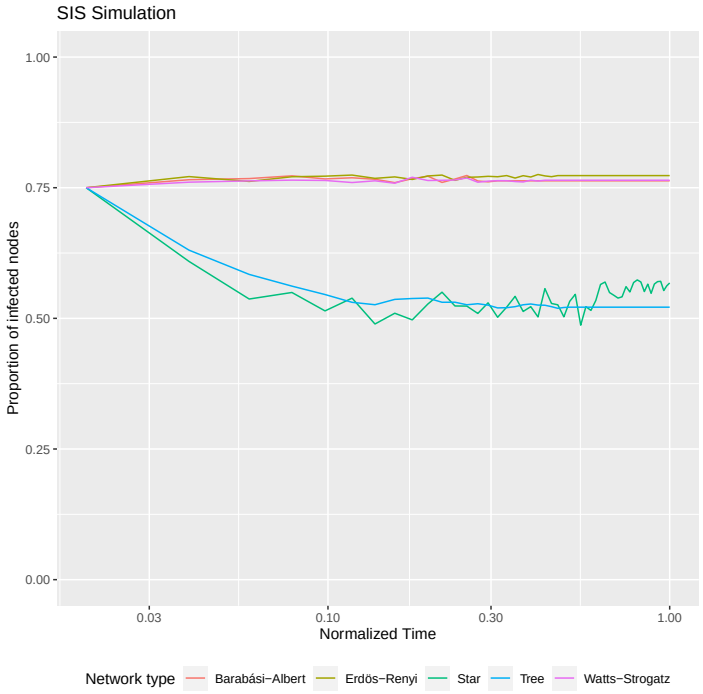

Figure 5: All networks with an initial infected population of 0.75

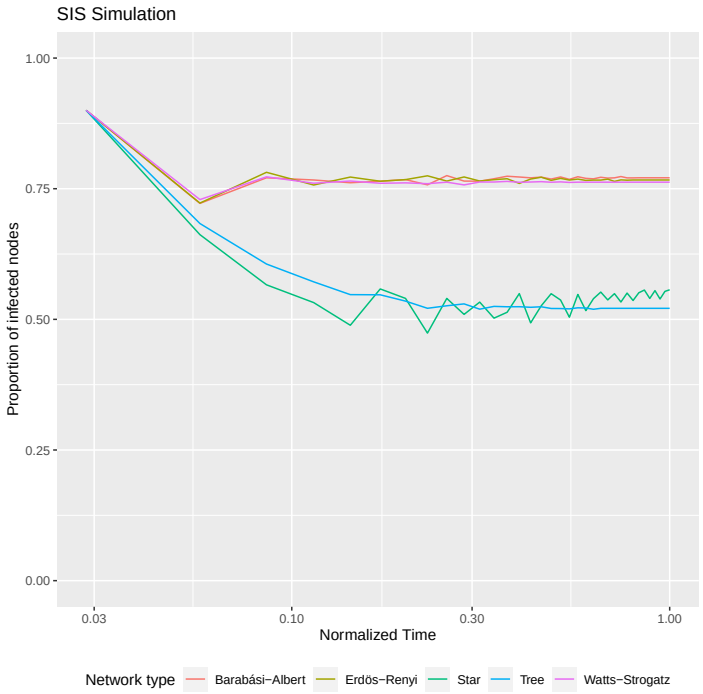

Figure 6: All networks with an initial infected population of 0.90

B Boxplot of leading eigenvalues on different networks,

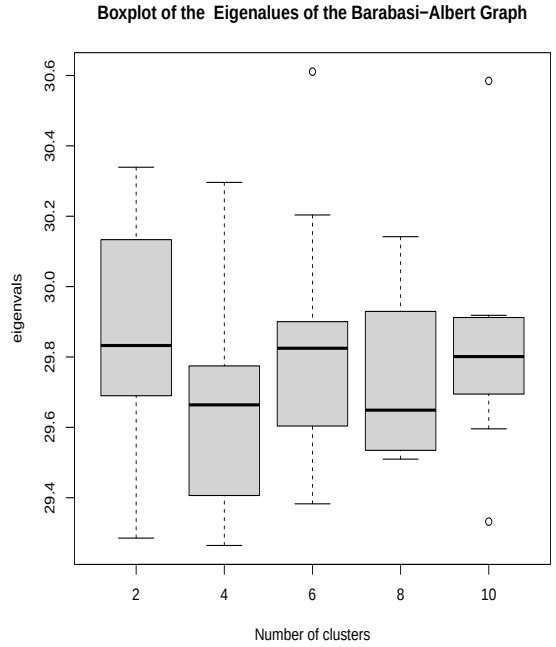

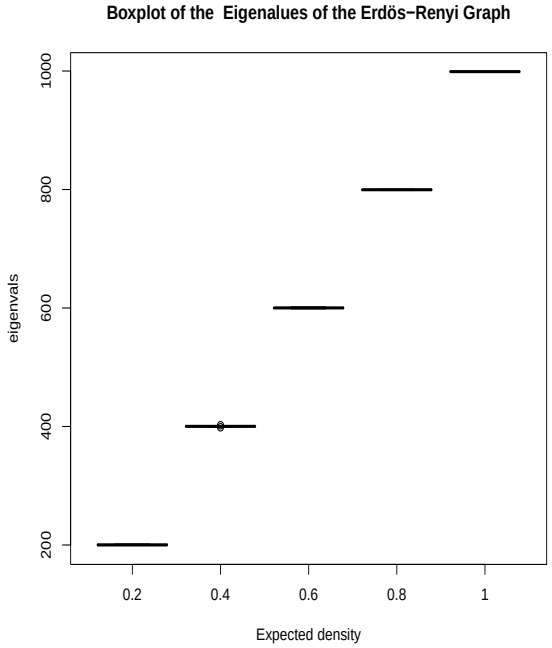

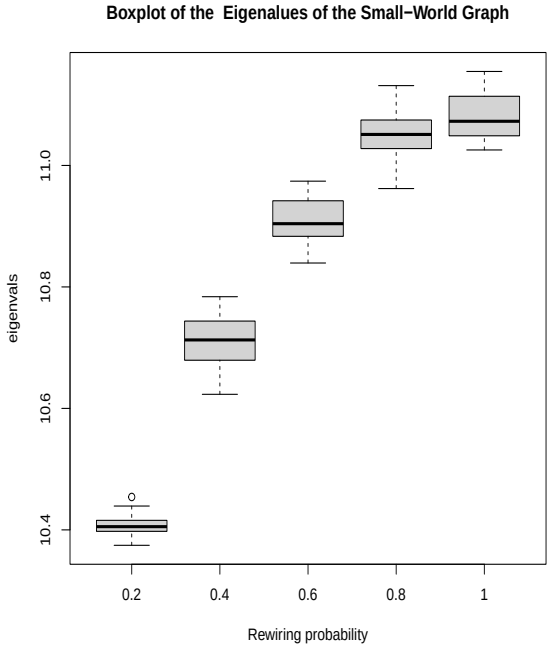

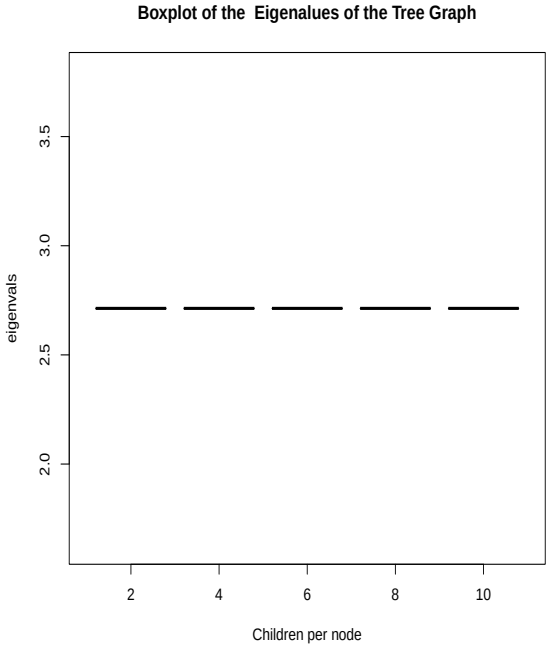

C Erdös-Renyi Plots

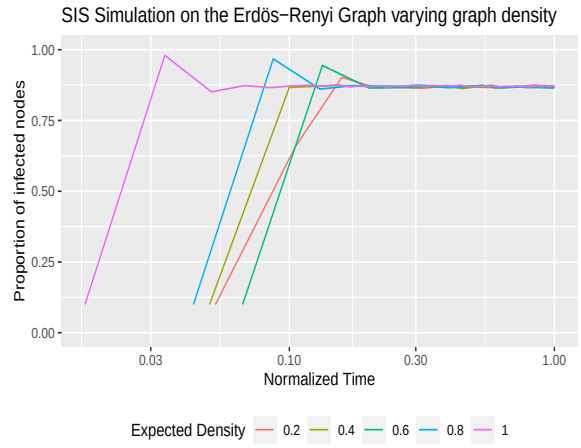

(a) γ=0.15

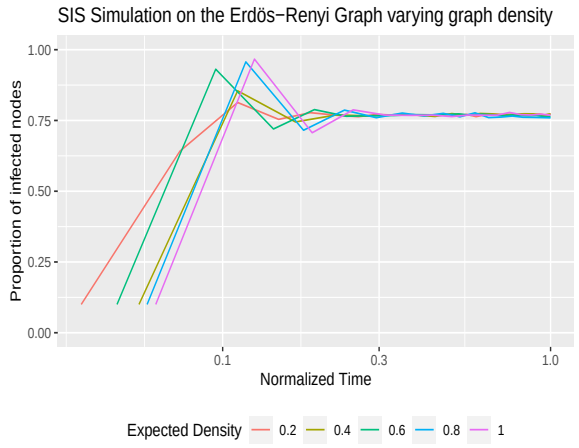

(b) γ=0.3

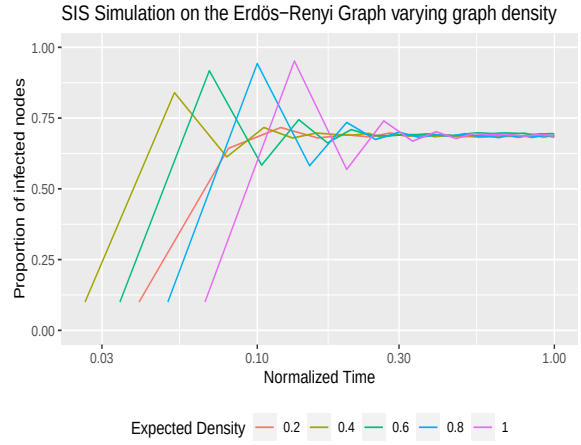

(c) γ=0.45

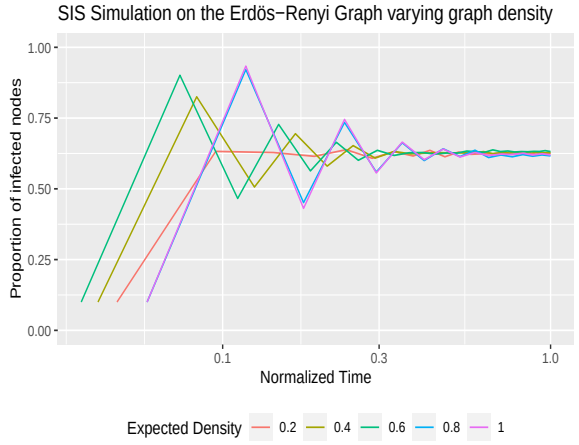

(d) γ=0.6

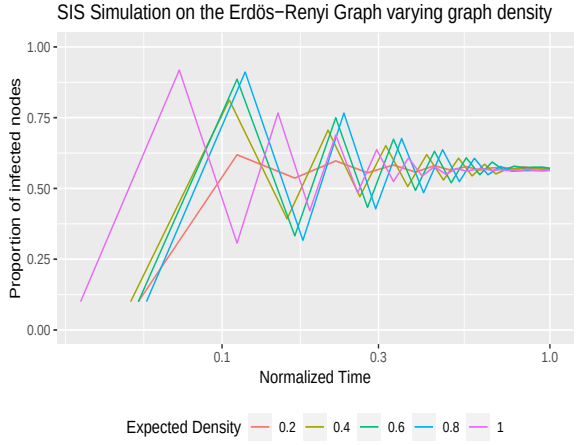

(e) γ=0.75

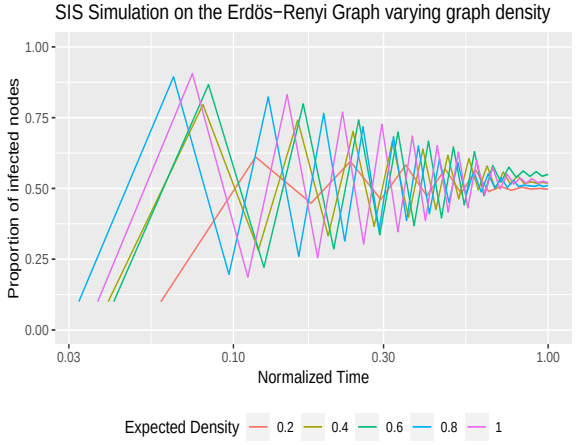

(f) γ=0.9

Figure 8: Above the threshold

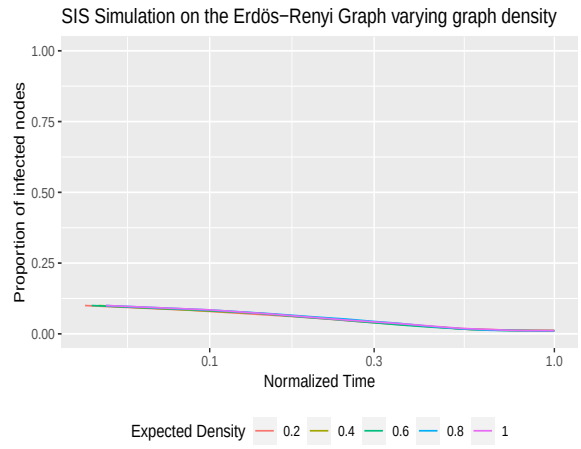

(a) γ=0.15

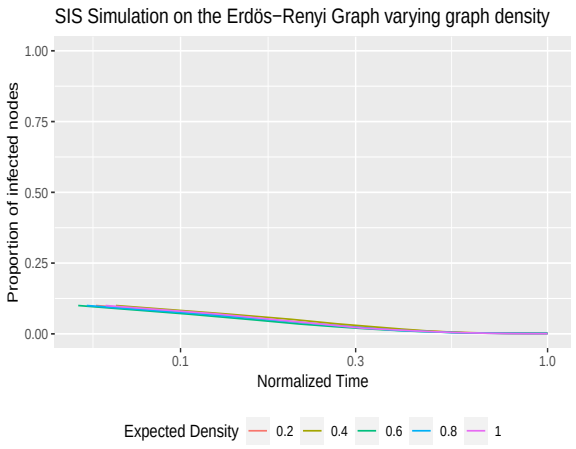

(b) γ=0.3

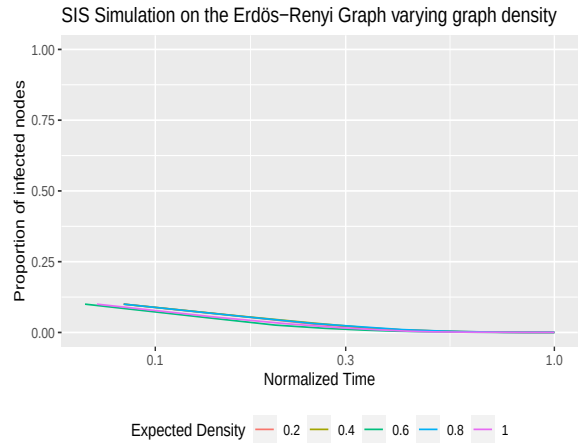

(c) γ=0.45

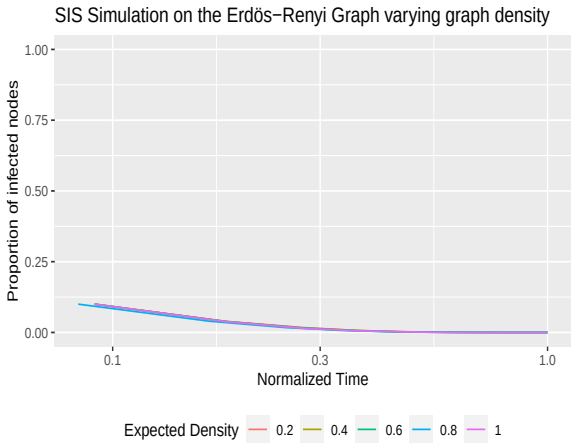

(d) γ=0.6

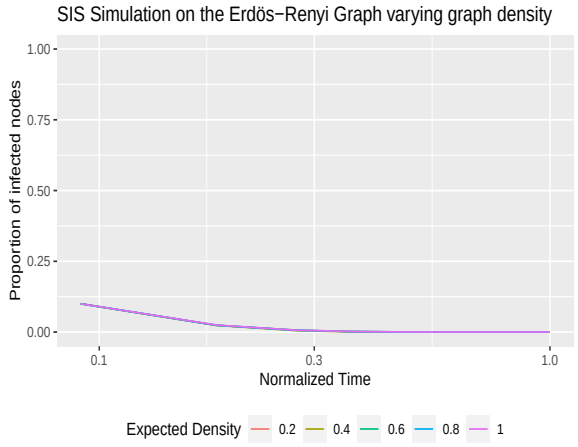

(e) γ=0.75

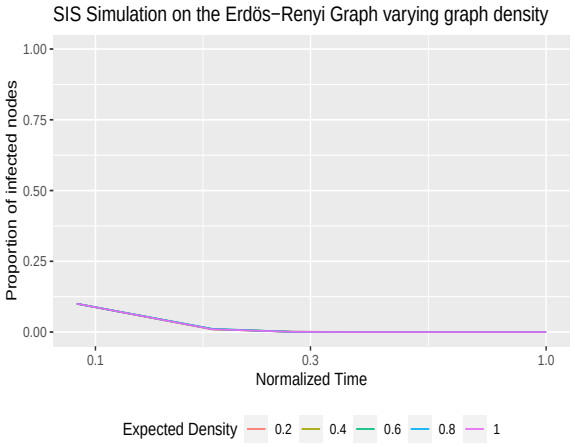

(f) γ=0.9

Figure 9: Below the threshold

D Barabási-Albert Plots

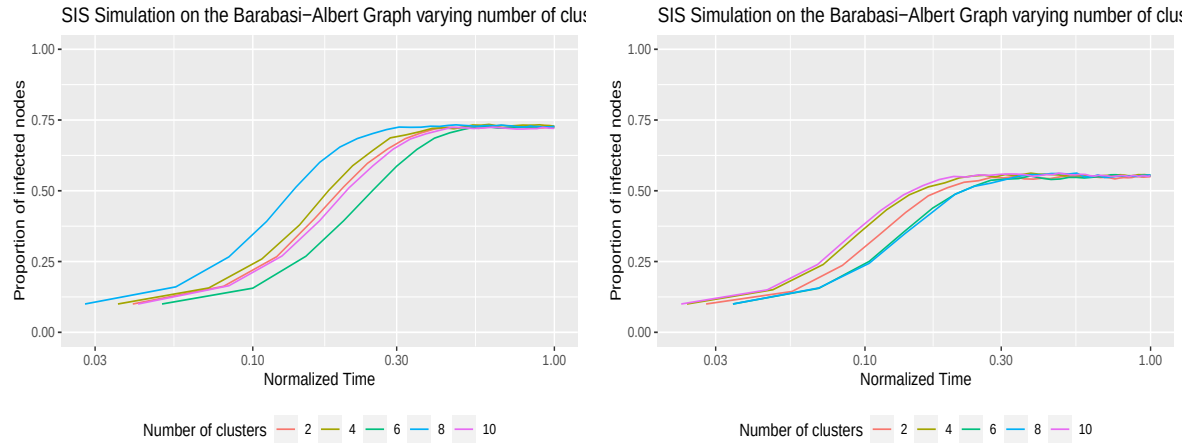

(a) γ=0.15

(b) γ=0.3

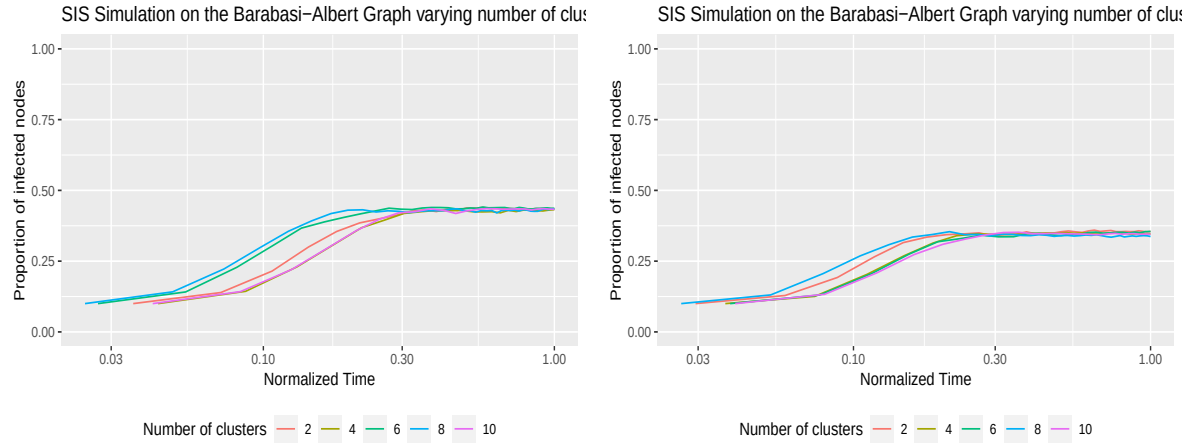

(c) γ=0.45

(d) γ=0.6

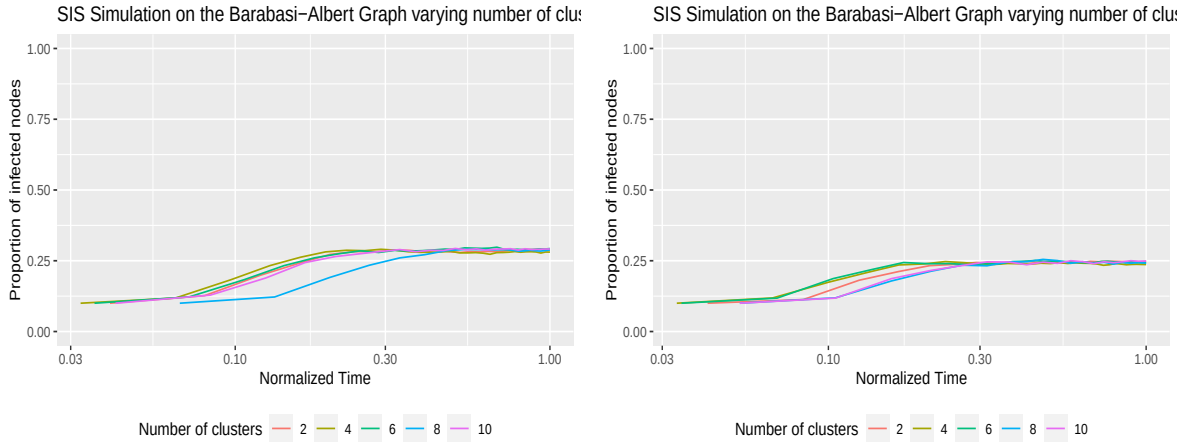

(e) γ=0.75

(f) γ=0.9

Figure 10: Above the threshold

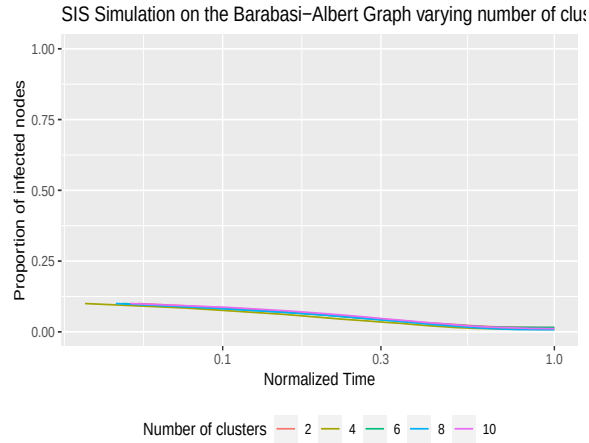

(a) γ=0.15

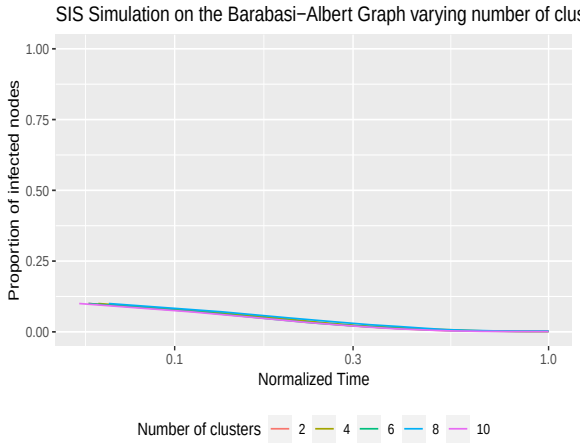

(b) γ=0.3

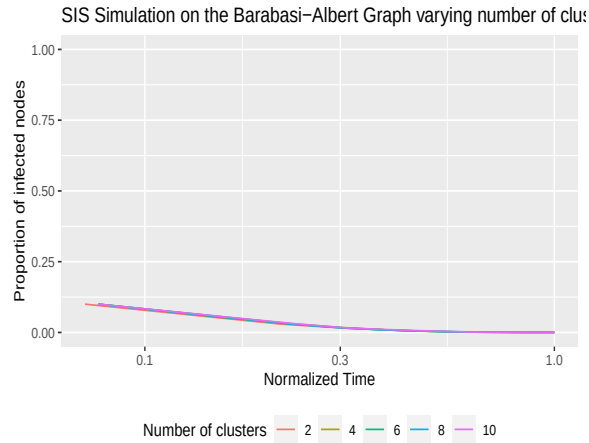

(c) γ=0.45

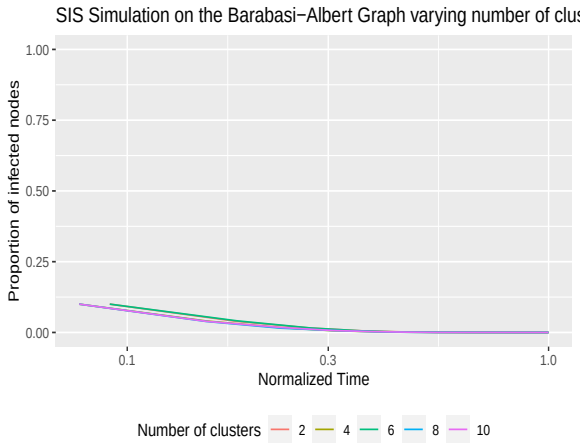

(d) γ=0.6

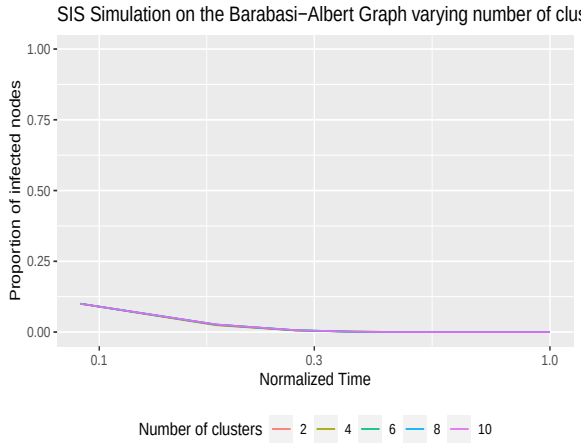

(e) γ=0.75

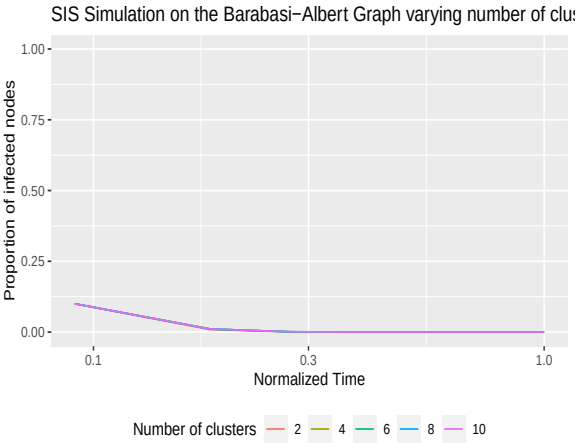

(f) γ=0.9

Figure 11: Below the threshold

E Small-World Plots

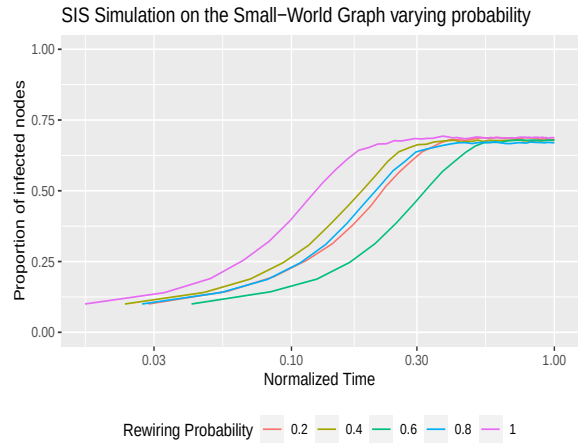

(a) γ=0.15

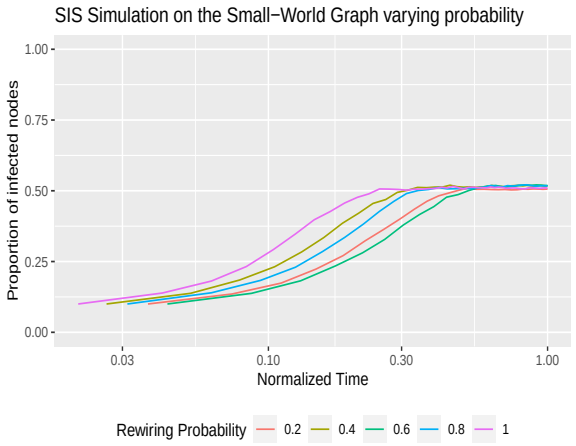

(b) γ=0.3

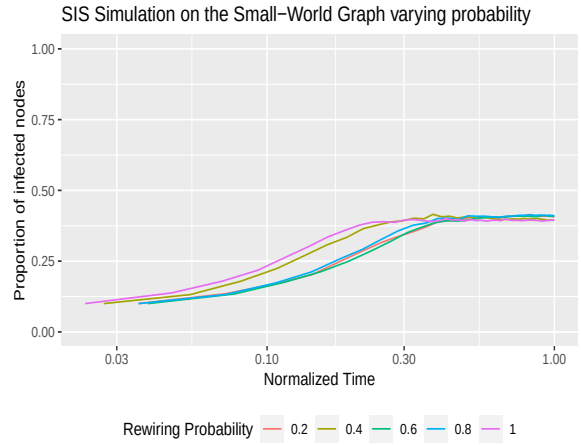

(c) γ=0.45

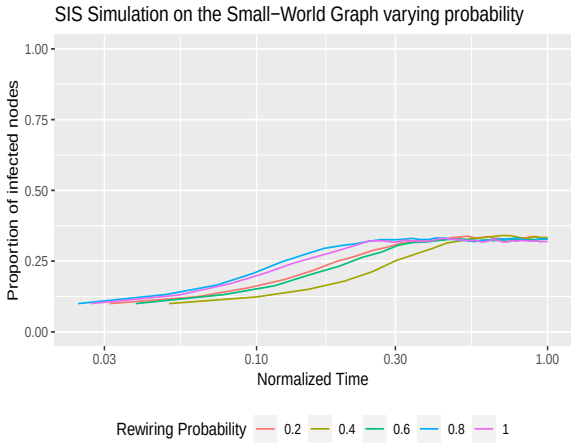

(d) γ=0.6

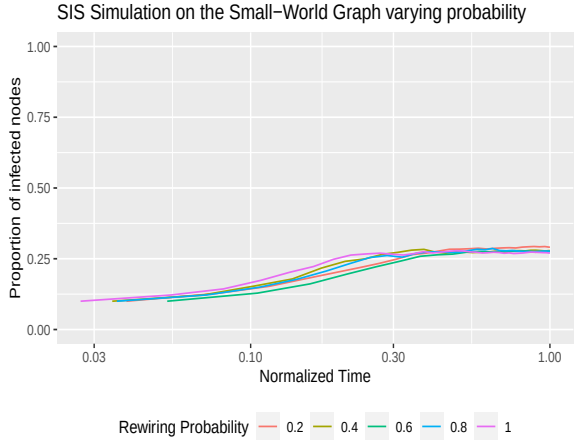

(e) γ=0.75

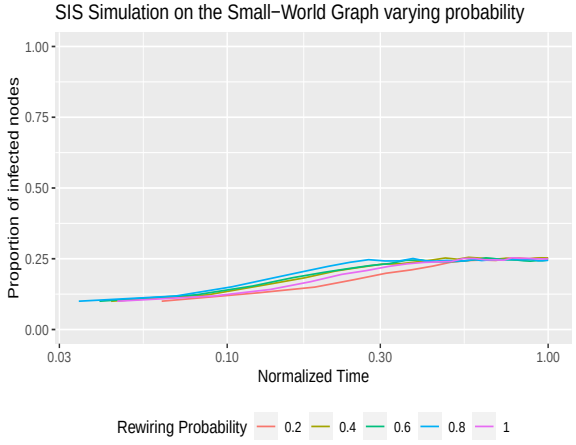

(f) γ=0.9

Figure 12: Above the threshold

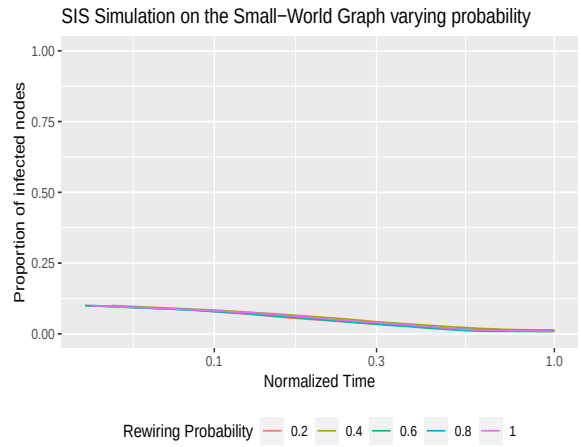

(a) γ=0.15

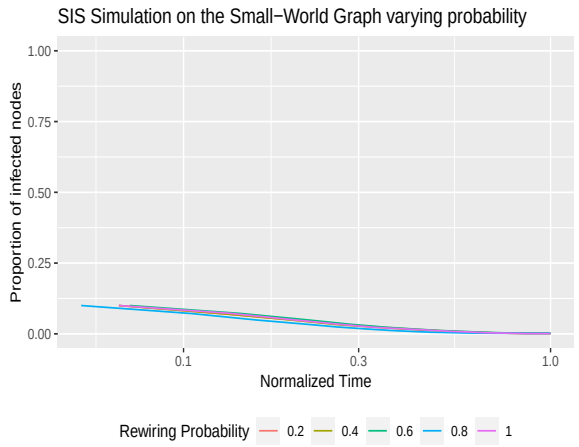

(b) γ=0.3

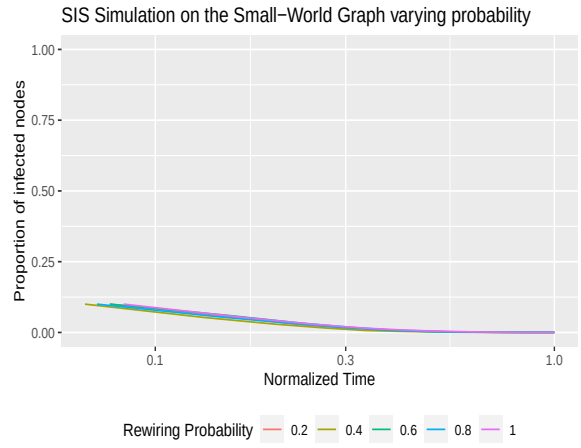

(c) γ=0.45

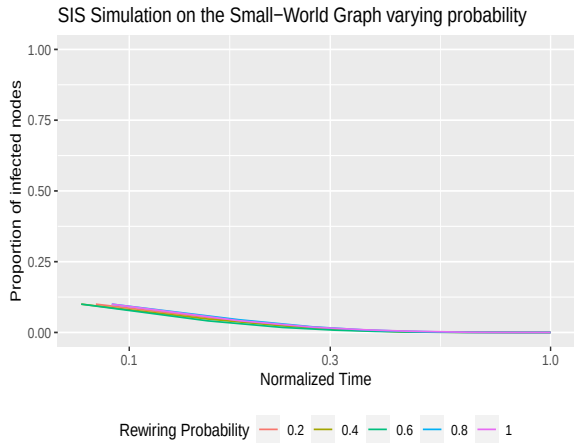

(d) γ=0.6

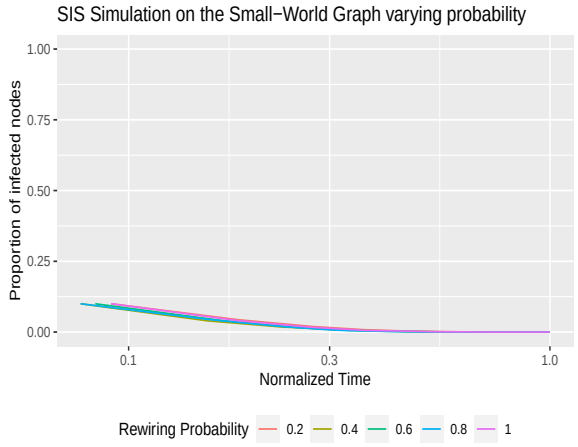

(e) γ=0.75

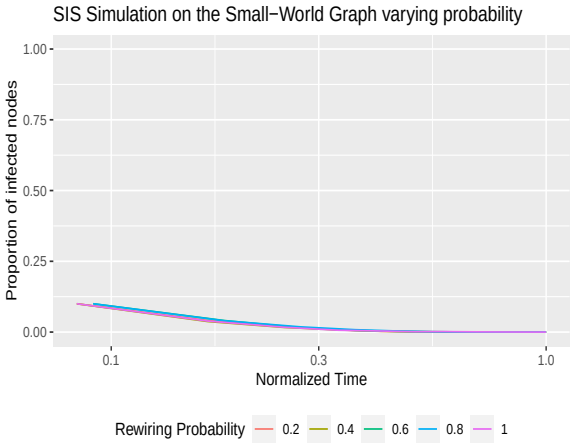

(f) γ=0.9

Figure 13: Below the threshold

F Star Plots

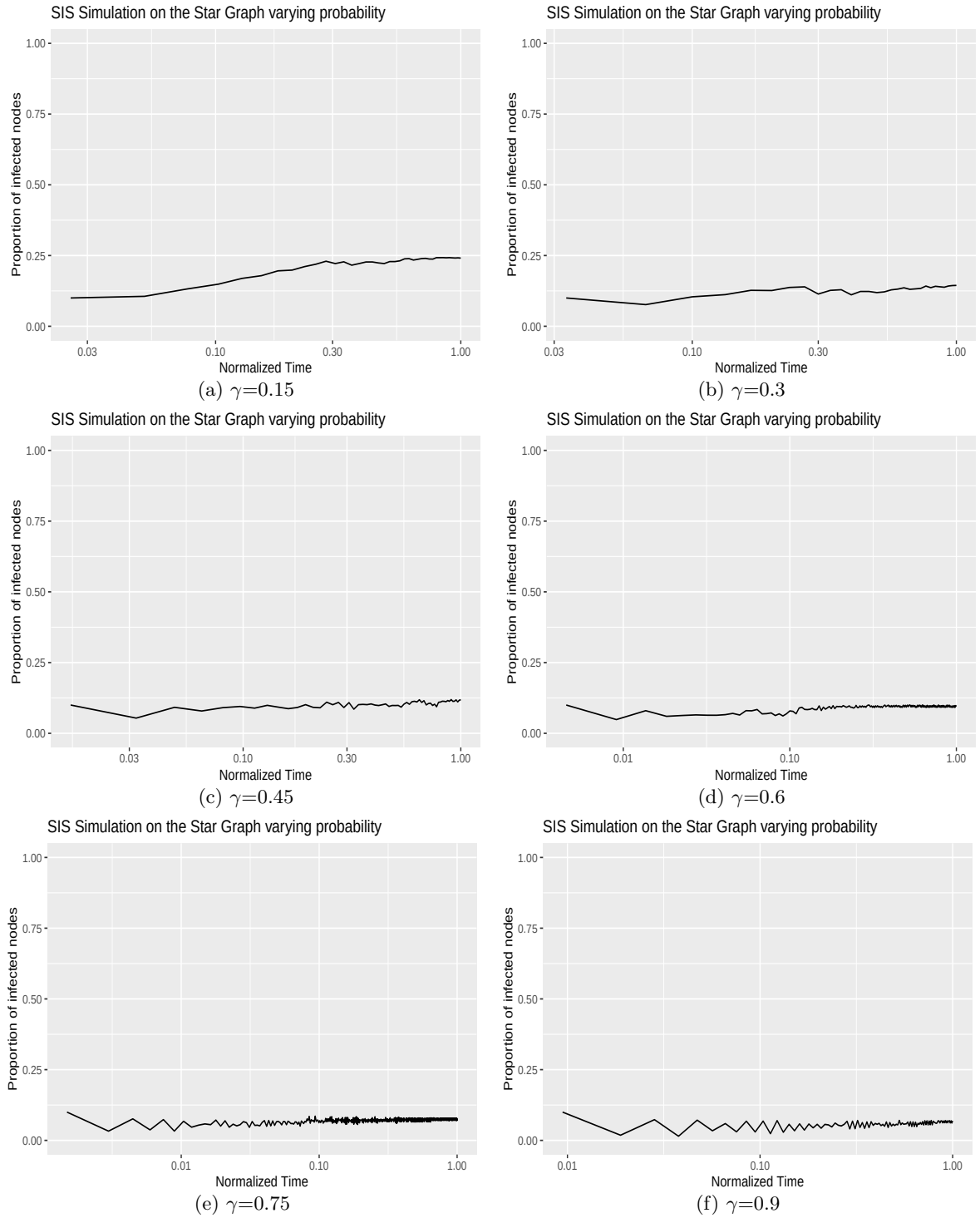

(a) γ=0.15 (b) γ=0.3

(c) γ=0.45 (d) γ=0.6

(e) γ=0.75 (f) γ=0.9

Figure 14: Above the threshold

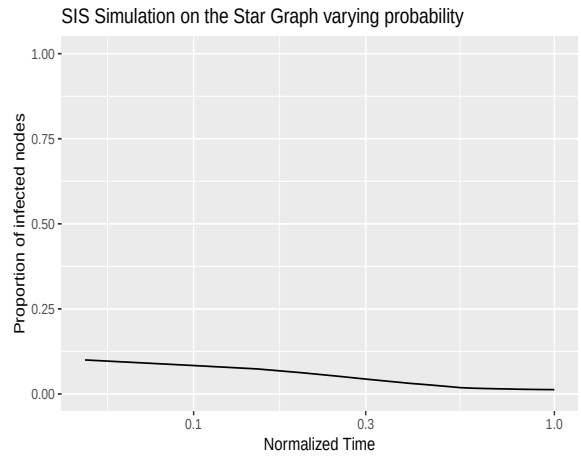

(a) γ=0.15

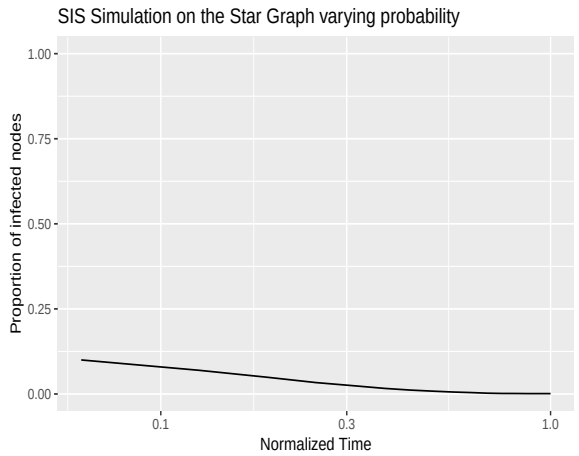

(b) γ=0.3

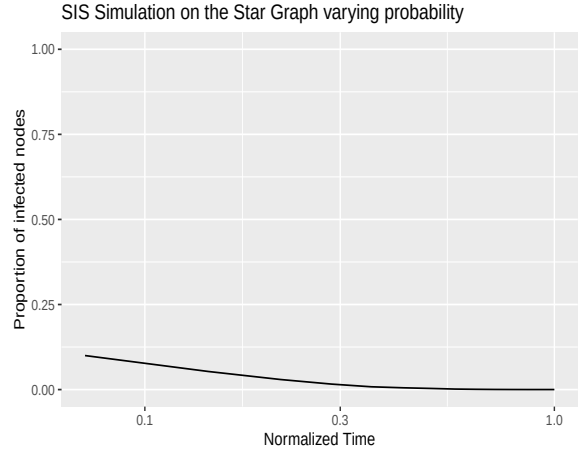

(c) γ=0.45

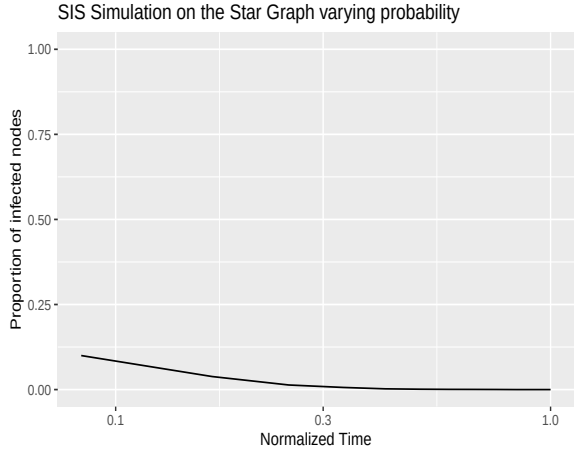

(d) γ=0.6

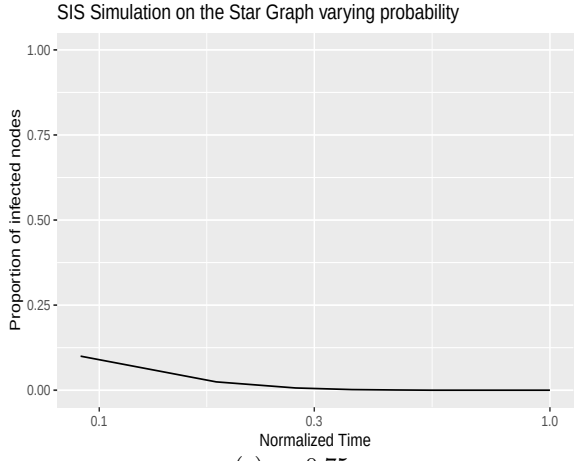

(e) γ=0.75

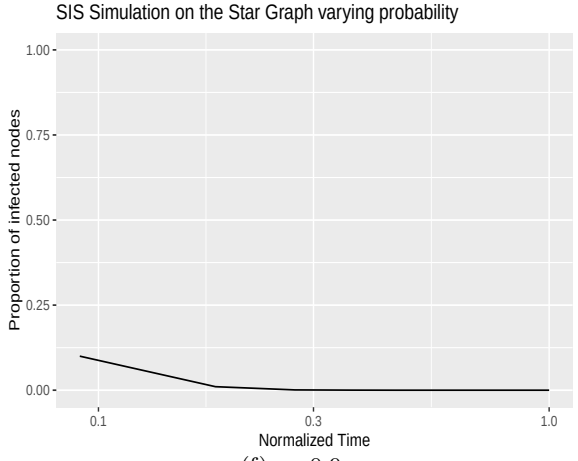

(f) γ=0.9

Figure 15: Below the threshold

G Tree Plots

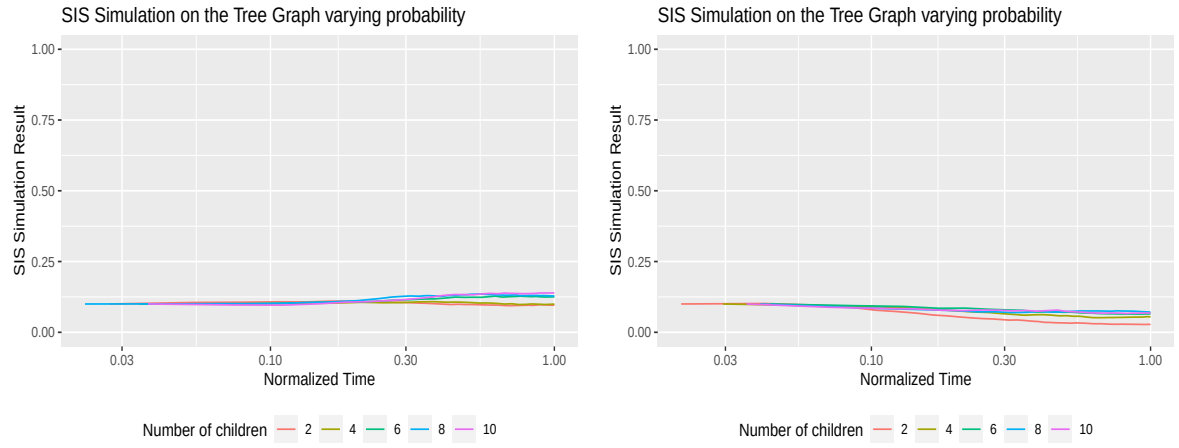

(a) γ=0.15

(b) γ=0.3

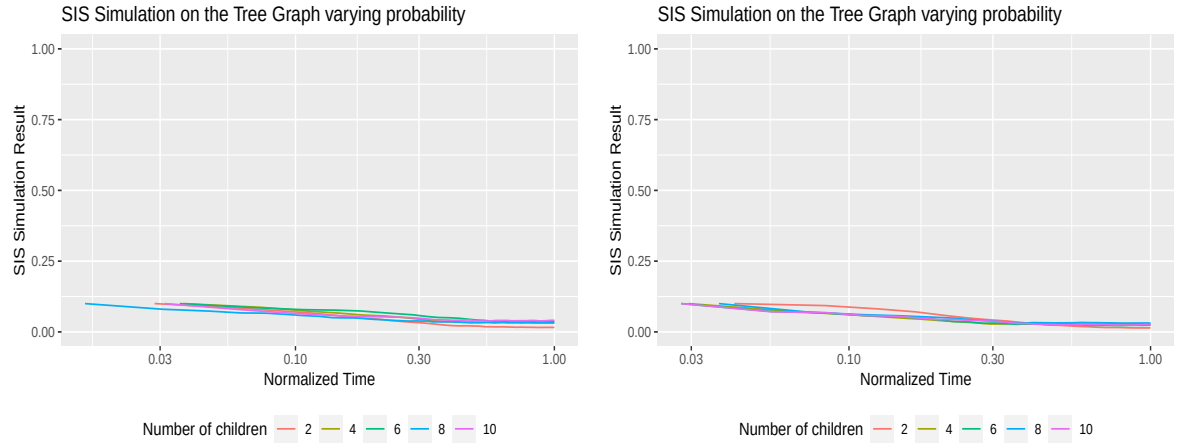

(c) γ=0.45

(d) γ=0.6

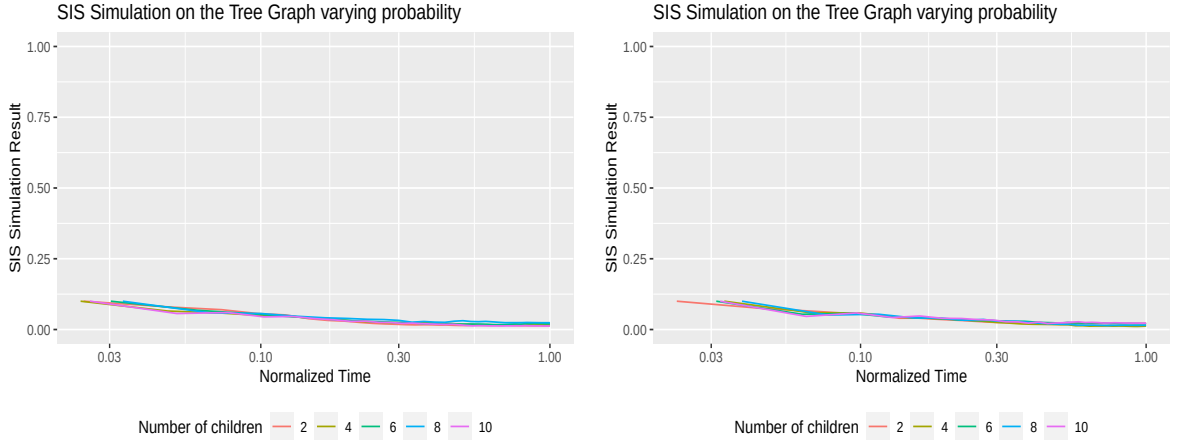

(e) γ=0.75

(f) γ=0.9

Figure 16: Above the threshold

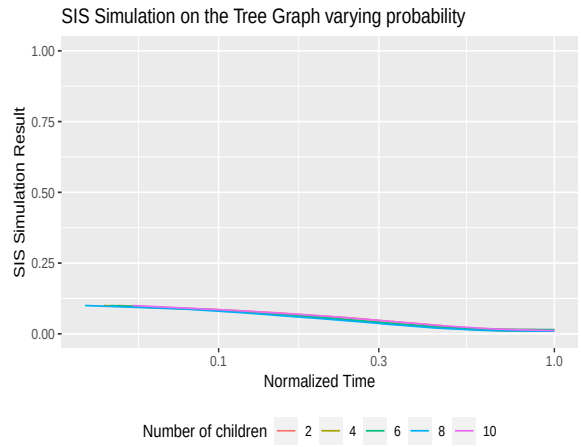

(a) γ=0.15

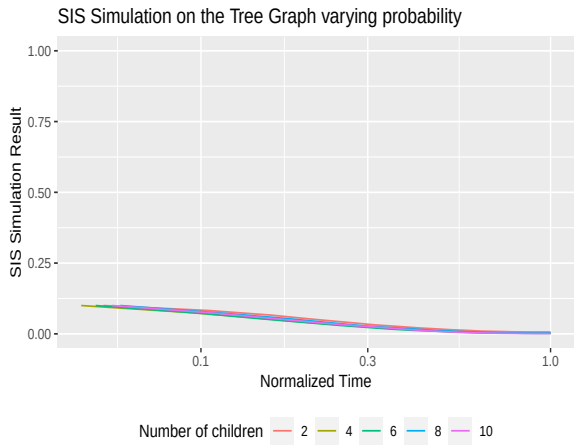

(b) γ=0.3

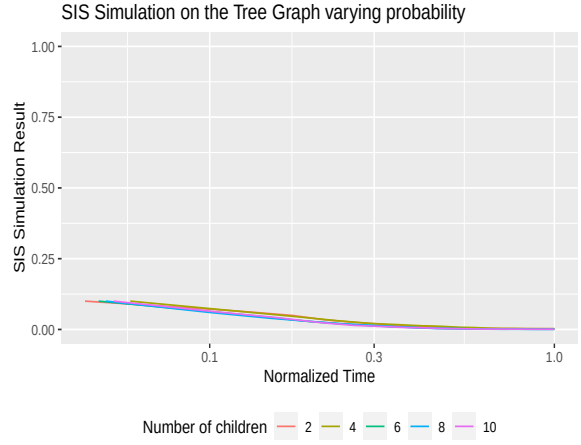

(c) γ=0.45

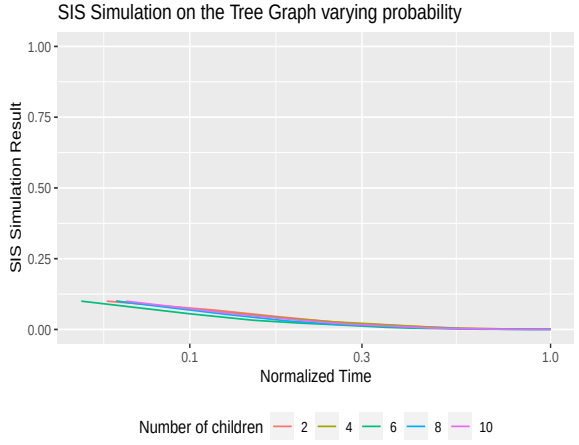

(d) γ=0.6

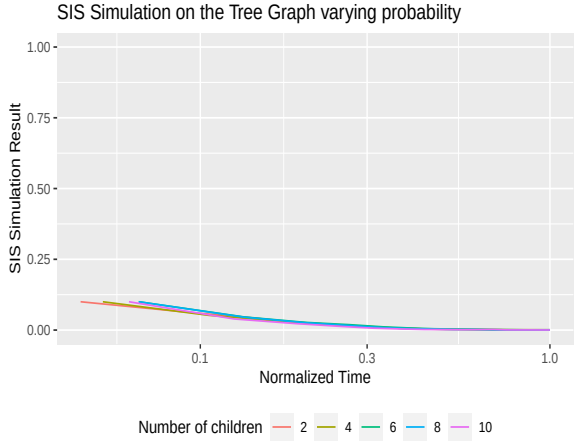

(e) γ=0.75

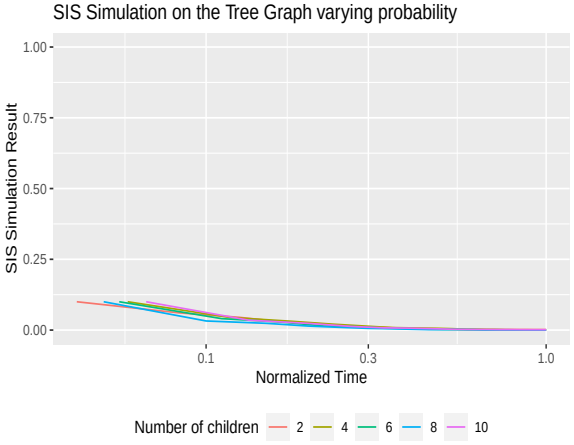

(f) γ=0.9

Figure 17: Below the threshold